Title

Three-dimensional reduced graphene oxide architecture embedded palladium nanoparticles as highly active catalyst for the Suzuki—Miyaura coupling reaction

Journal

Materials Chemistry and Physics, 148(1-2)

ISSN

0254-0584

Authors

Wang, Xizheng

Chen, Wufeng

Yan, Lifeng

Publication Date

2014-11-01

DOI

10.1016/j.matchemphys.2014.07.018

Materials Chemistry and Physics 148 (2014) 103–109

Contents lists available at ScienceDirect

Materials Chemistry and Physics

journal homepage: www.elsevier.com/locate/matchemphys

Three-dimensional reduced graphene oxide architecture embedded palladium nanoparticles as highly active catalyst for the Suzuki–Miyaura coupling reaction

Xizheng Wang, Wufeng Chen, Lifeng Yan*

CAS Key Laboratory of Soft Matter Chemistry, Hefei National Laboratory for Physical Sciences at the Microscale, and Department of Chemical Physics, University of Science and Technology of China, Hefei 230026, PR China

HIGHLIGHTS

- 3D architecture of graphene embedded palladium nanoparticles has been prepared.
- The obtained composites are three-dimensional, porous, light-weight.
- The size of the Pd nanoparticles is 5–9 nm.
- The nanocomposite showed highly catalytic activity for Suzuki–Miyaura coupling reaction.
- The method can be used to prepare other metal nanoparticles-rGO 3D composites.

GRAPHICAL ABSTRACT

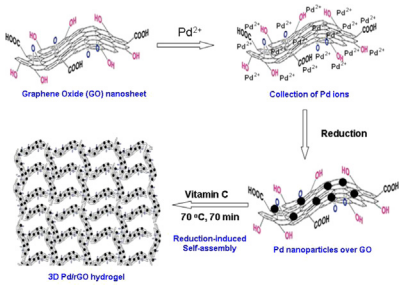

ARTICLE INFO

Article history:
Received 19 March 2014
Received in revised form
9 June 2014
Accepted 12 July 2014
Available online 1 August 2014

Keywords:
Inorganic compounds
Nanostructures
Chemical synthesis
Surface properties

ABSTRACT

3D architecture of graphene embedded palladium nanoparticles has been prepared by a simple two-steps method. At first, Pd nanoparticles was anchored and growth over graphene oxide (GO) nanosheets in aqueous solution using different reducing agents. Then, the as-prepared Pd/GO nanosheets were reduced by Vitamin C, and the hydrogel of Pd/reduced GO (rGO) was formed *via* a reduction-inducing self-assembly. The obtained 3D Pd/rGO architecture was studied by means of XRD, XPS, TGA, AFM, BET, and elemental analysis, and it revealed that the obtained composites are three-dimensional, porous, light-weight with a homogeneous dispersion of Pd nanoparticles in size of 5–9 nm. The as-prepared 3D Pd/rGO nanocomposite showed highly catalytic activity for Suzuki–Miyaura coupling reaction.

1. Introduction

Carbon-supported nanoparticles of metals or metal oxides have wide applications in the field of catalysis [1], energy conversion and storage [2], and biomedicine [3]. As a member of the carbon family, graphene has recently attracted much attention for its unique electronic properties, excellent mechanical properties, and superior thermal properties [4,5]. Supporting metal nanoparticles on graphene nanosheets could provide a large surface area and thermal stability for potential applications [6,7]. As compared to two-dimensional graphene, three-dimensional (3D) graphene architecture provides higher specific surface area and large pore volume,

* Corresponding author. Tel.: +86 551 63606853; fax: +86 551 63603748.
E-mail address: lfyan@ustc.edu.cn (L. Yan).

http://dx.doi.org/10.1016/j.matchemphys.2014.07.018
0254-0584/

and a multiple lattice-layered graphitic structure, which is an idea support for metals or metal oxides for catalysis, fuel cells, chemical sensors, and hydrogen storage [8–13].

In the field of catalysis, chemically exfoliated graphene oxide (GO) and reduced graphene oxide (rGO) have been used as supporting materials for active species [14]. From a theoretical point of view, graphene provides the ultimate two-dimensional model of a catalytic support. Unfortunately, the physical properties of graphene in its powder form do not allow it to be used in industrial reactors, such as fixed- or fluidized-bed reactors. Several strategies had been envisaged to overcome the difficulty, pelletization or gelation of graphene maybe the value choices [14,15]. Constructing of 3D architectures of graphene had been reported by different methods. Such as self-assembly, organic sol–gel reaction, hydrothermal treatment, template guide growth, and LightScribe patterning technology etc [8,16]. The as-prepared 3D graphene architectures not only have the inherent properties of graphene, but also exhibit improved functions resulting from their special microstructures, and the controlled meso-, micro- and nano-structures are important for catalysis, flexible electronics, supercapacitors, Li ion battery, hydrogen storage, and sensors. In our previous studies, the nanosheets of graphene oxide can be assembled into 3D graphene hydrogel by a reduction-induced *in situ* self-assembly process [16], especially it can form hydrogel of graphene/inorganic nanoparticles, and it provides chances for fabricate new 3D architecture of graphene/nanoparticles of metal or metal oxides for catalysis [13,17].

Decorating graphene with nanoparticles of metal or metal oxides has been paid much attention due to their enhanced potential applications, especially in the field of catalysis [14,18]. Well dispersed metal nanoparticles over graphene had been reported, including metal nanopartilces of Au, Pt, Pd, Ag, Ru, Rh, Ir, Fe, Cu, Ni, Co, Ge, and Sn, or metal oxide nanoparticles of TiO_2, ZnO, SnO_2, Fe_3O_4, MnO_2, Co_3O_4, RuO_2, MoO_3 and ZrO_2. Studies using first-principles density-functional theory with the generalized gradient approximation revealed that the adsorption of Au, Ag, and Cu was considered as physisorption, whereas Co, Ni, Pt and Pd covalently bonded to graphene [14,19].

It is well known, Pd is an efficient catalyst for C–C coupling reactions, such as Mizoroki–Heck reaction, Suzuki–Miyaura reaction. R. Heck, E. Negishi, and A. Suzuki had the 2010 Noble Price in Chemistry for their groundbreaking work [20]. However, the use of Pd-based catalysts in homogeneous conditions has limited their commercial application for the requirement of the recovery of Pd ions. Deposited Pd nanoparticles on a support can resolve this problem, and Mulhaupt et al. reported the immobilization of Pd nanoparticles on graphite oxide and its functionalized graphene derivatives, and found that they are highly active catalysts for the Suzuki–Miyaura coupling reaction [21]. El-shall et al. recently reported a laser assistant method to prepare Pd-partially reduced graphene oxide for C–C cross coupling reactions [22]. Other methods had also reported for preparation of Pd nanoparticles/graphene for C–C coupling reaction, and all of them showed considerable efficient catalysis ability that commercial Pd/C catalyst [21,23–30]. However, all the studies directly utilized 2D graphene of GO sheets as the support, what will happen if 3D graphene architecture is used as the porous support for Pd nanoparticles? [27,31].

Here, we try to prepare a new hydrogel of graphene and Pd nanoparticles by a reduction-induced *in situ* self-assembly of Pd nanoparticles anchored nanosheets of graphene oxides in aqueous suspension. Then the as-prepared Pd/rGO hydrogel was dried and worked as the catalyst for Suzuki–Miyaura coupling reaction, and a high catalysis activity was detected.

2. Experimental

2.1. Materials

Graphite powder, natural briquetting grade, about 100 mesh, 99.9995% (metals basis) was purchased from Alfa Aesar. Analytical grade Vitamin C, bromobenzene, iodobenzene, phenyl boronic acid, ethanol, K_2PdCl_4, $PdCl_2$, Na_2CO_3, $NaNO_3$, $KMnO_4$, Na_2SO_4, 98% H_2SO_4, 30% H_2O_2 aqueous solution, ammonia aqueous solution, and hydrochloric acid aqueous solution were purchased from Shanghai Chemical Reagents Company, and were used directly without further purification. Ultra-pure water (18 MΩ) was produced by a Millipore System (Millipore Q, USA).

2.2. Preparation of Pd nanoparticles over GO nanosheets

Aqueous suspension of GO nanosheets was prepared by the oxidation of high purity graphite powder according to the modified Hummer method [32]. GO powders can be obtained after it was washed by ultrapure water followed by freeze drying. For the preparation of Pd nanoparticles over GO, Vitamin C was used as reducing regent. In brief, 0.13 g of GO powder was dispersed into 33 ml of ultrapure water at room temperature, and 0.5 ml of Vitamin C (2.8 mg ml^{-1}) was added drop wise, and the mixture was stirred for 30 min at room temperature. Next, the mixture was filtrated and the cake was washed by ultrapure water and acetone, respectively. After freeze-drying a brown powder was obtained, and it was reduced by bubbling hydrogen gas (40 ml min^{-1}) for 30 min or 5 h in ethanol (10 ml). After evaporation of the ethanol, powder of Pd nanoparticles/GO was made.

2.3. Preparation of Pd/rGO 3D architecture

The above as-prepared Pd/GO was used as feed stocks for the 3D architecture preparation. For the Pd/GO prepared by Vitamin C reduction, 1.5 ml of Vitamin C (0.24 g ml^{-1}) was added into the mixture by drop under stirring, and then the mixture was heated up to 70 °C for 70 min without stirring, and a black hydrogel was formed after the reaction [13]. At the end, black columns of 3D hydrogel of Pd/rGO were formed *via* a reduction-induced self-assembly of GO nanosheets. The as-prepared Pd/rGO hydrogel was dialyzed against ultrapure water for 2 days to remove residual free compounds, and black 3D Pd/rGO architectures were obtained after freeze-drying. The total synthesis process was illustrated in Scheme 1.

2.4. Characterization

The morphologies of the hydrogel were characterized by SEM-EDX system (Superscan SSX-550, Shimazu). The thermal properties of the samples were recorded by a thermogravimeter (TGA, DTA-50, Shimazu), and all of the measurements were performed in nitrogen gas over a temperature range of 30–800 °C with a ramp rate of 5 °C min^{-1}. Wide-angel X-ray diffraction (XRD) analyses were carried out on an X-ray diffractometer (D/MAX-1200, Rigaku Denki Co. Ltd., Japan). X-ray photoelectron spectroscopy (XPS) was recorded on an Escalab MK II photoelectron spectrometer (VG Scientific Ltd., United Kingdom). A commercial atomic force microscope (AFM, Nanoscope IIIa; Digital Instruments, Santa Barbra, CA), equipped with a J scanner was used to measure the morphologies and thicknesses of the samples. Si_3N_4 tip (Nanoprobes, Digital Instruments Inc.) was exercised by the contact mode. Scan rates ranged from 1.0 to 2.4 Hz. The Brunauer–Emmett–Teller (BET) specific surface area and porous structure characteristics of the hydrogels were investigated by nitrogen isothermal adsorption. (ASAP 2020M+C, Micromeritics).

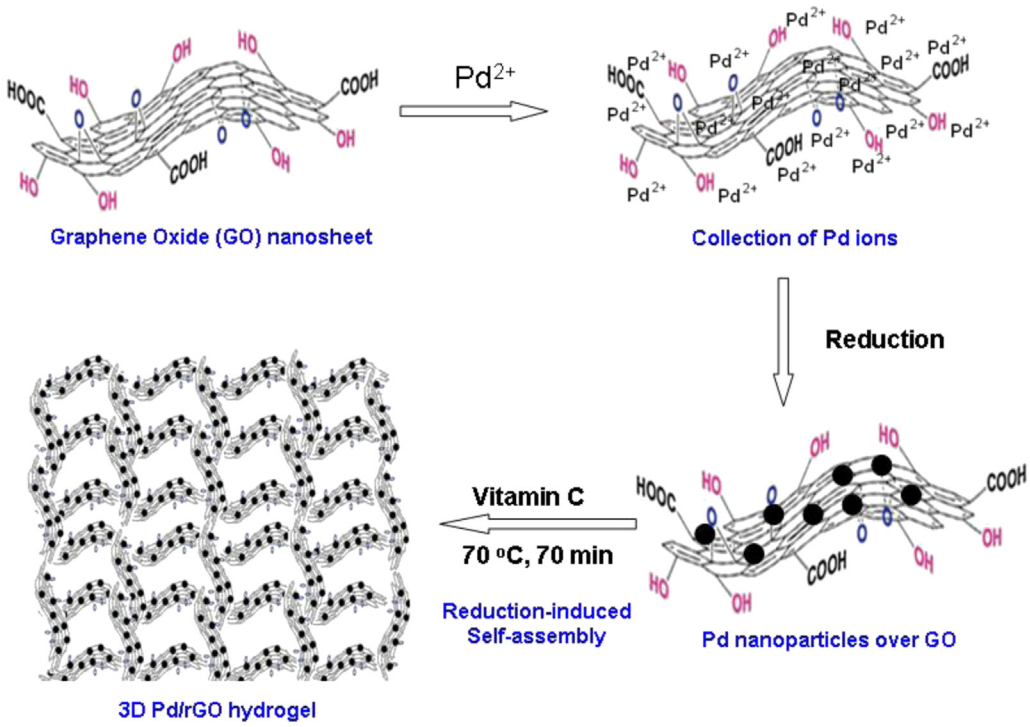

Scheme 1. An illustration of the formation of Pd nanoparticles over GO nanosheet, and sequent reduction and *in situ* self-assembly for the formation of 3D Pd/rGO hydrogel.

2.5. General procedures for the Suzuki reaction

As shown in Scheme 2, Bromobenzene (0.15 g, 0.98 mmol) or iodobenzene (0.16 g, 0.79 mmol) were dissolved in a mixture of 7.2 ml of H_2O:EtOH (1:1), and to this mixture, phenyl boronic acid (0.12 g, 1.0 mmol) and sodium carbonate (0.19 g, 1.8 mmol) were added. Powder of 3D Pd/rGO catalyst (4.0 mg) was then added, and the autoclave, and it was sealed and stirred at 80 °C for 4 h. After reaction, the products were analyzing by means of HPLC.(LC-20AD, Shimadzu). In addition, 4-methoxypheneboronic acid and 4-bromo-1,2-(methylene dioxy)benzene (0.95 mmol) were used as different substrates for the Suzuki reaction under the catalysis of Pd/rGO, and the mixture of water and ethanol (1:1,v:v) was used as the solvent, and the reaction were carried out at temperature from room temperature to 80 °C for 4 h in the presence of sodium carbonate.

3. Results and discussion

Fig. 1a shows the typical AFM height image of the as-formed Pd nanoparticles over the surface of a GO nanosheet, and the section line analysis (Fig. 1b) clearly shows that the nanosheet of GO is in the thickness of about 1.4 nm and in size of micrometers, and the surface covered by plenty of nanoparticles in height of about 4–8 nm, and they are distributed homogeneously. After the Pd/GO aqueous suspension was reduced by Vitamin C at 70 °C, a black cylinder hydrogel was obtained, as shown in Fig. 1c. Fig. 1d shows the TEM image of the Pd/GO nanosheet, and clearly some Pd nanoparticles in size about 5–10 nm are formed on the surface of GO nanosheets with a homogeneous dispersion, and the result is consistent to that of AFM measurement. After it was reduced and a 3D architecture formed, and Fig. 1e shows the TEM image of the dried Pd/rGO hydrogel at the edge, and the overlap of the Pd/rGO nanosheets can be found, and the difference of the darkness of Pd nanoparticles (indicated by red (in the web version) or blue arrows) reveal the lengthways dispersion of Pd nanoparticles from surface to the inside of the rGO network.

Fig. 2a shows the SEM cross-section image of the dried Pd/rGO hydrogel, and a 3D porous network can be observed. The presence of elements of palladium, carbon and oxygen in the hydrogel was confirmed by the EDX measurement (Fig. 2b), where carbon is mainly contributed from rGO framework, and oxygen is corresponds to the residual oxygen-containing group in rGO. The dried hydrogel is composition of 62.0 wt% of carbon and 5.4 wt% of palladium, indicating the formation of the composite hydrogel of Pd and rGO.

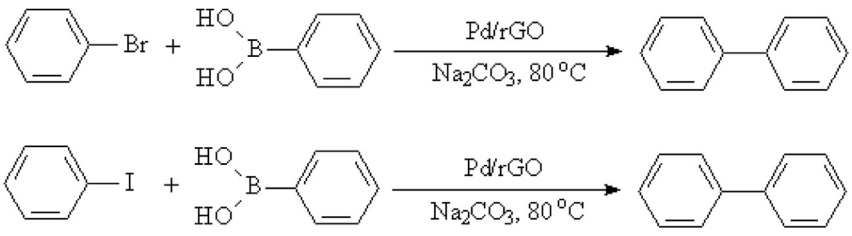

Scheme 2. Reaction route of Pd/rGO catalysis Suzuki–Miyaura coupling reaction.

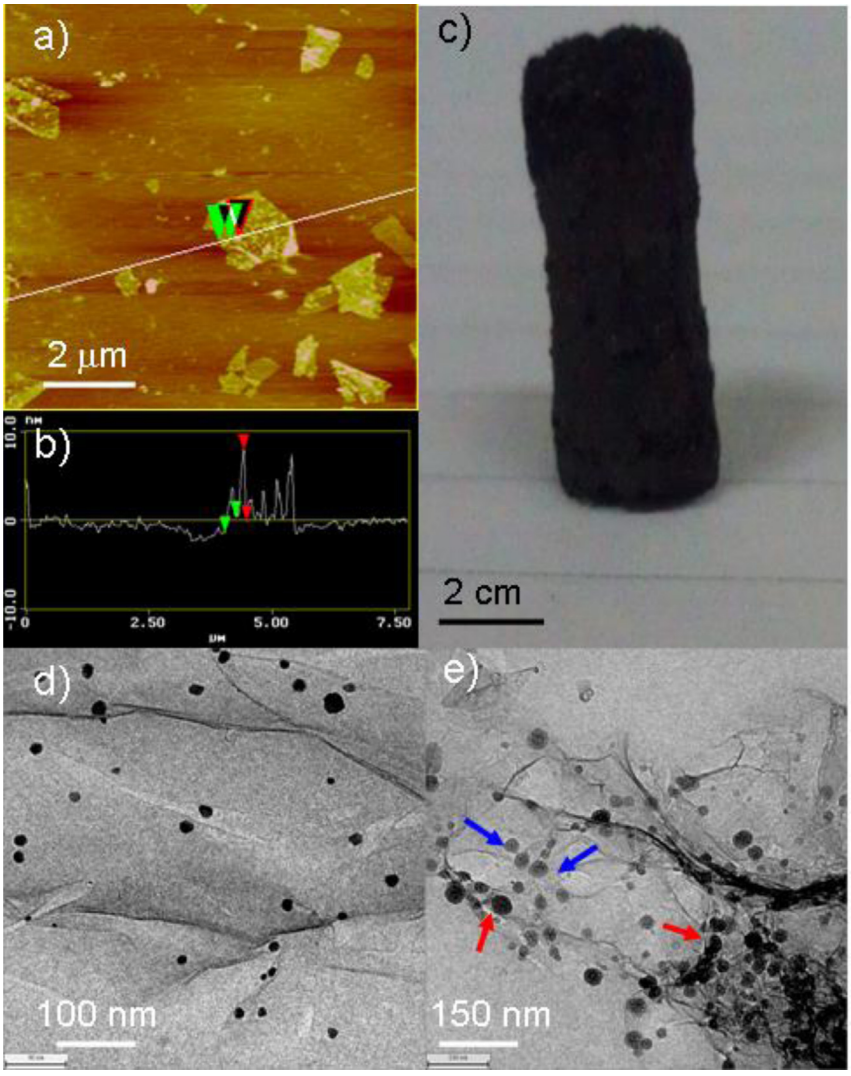

Fig. 1. a) AFM height image of Pd/GO nanosheet by depositing its aqueous suspension onto the surface of new cleaved mica. b) Section line analysis of the GO nanosheet and nanoparticles. c) Photoimage of the as-prepared dried Pd/rGO hydrogel. d) TEM image of the Pd nanoparticles on the surface of GO. e) TEM image of the Pd nanoparticles on the surface of rGO hydrogel.

Fig. 3 shows XPS spectra of the dried Pd/rGO hydrogel. Both C1s and Pd3d patterns were demonstrated. For Pd3d pattern, two main peaks locate at 338 eV and 343 eV, correspond to the Pd $3d^{5/2}$ and Pd $3d^{3/2}$ in palladium nanoparticles [26]. For C1s pattern, the main peak locates at 284.6 eV, corresponds to C═C/C–C species. In addition, a weak peak at 287 eV appears, which is attributed to oxygen-containing species of rGO, indicating an efficient reduction of GO during the formation of the Pd/rGO hydrogel [13].

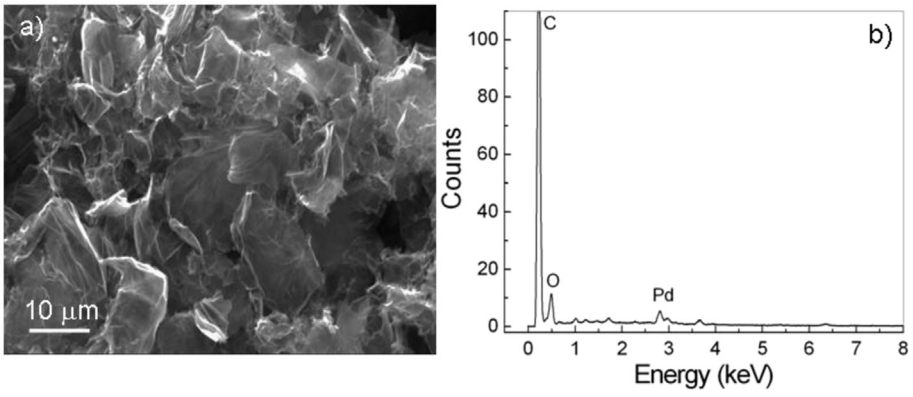

Fig. 2. SEM cross-section image (a) and EDS spectrum (b) of the dried Pd/rGO hydrogel.

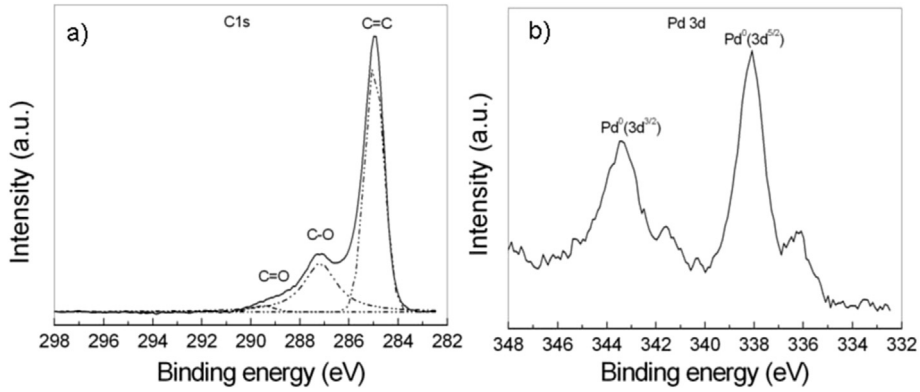

Fig. 3. XPS spectra of the dried Pd/rGO hydrogel: a) C1s pattern, b) Pd 3d pattern.

The thermal stability of GO, rGO, Pd/GO and Pd/rGO hydrogels have been investigated in nitrogen by TGA measurements. Fig. 4 shows the TG curves of them. For GO, there are two steps for mass losing on increasing the temperature. Mass loss is about 10% at around 100 °C, which can be attributed to the removal of adsorbed water. Mass loss at around 200 °C is about 40%, and was attributed to the decomposition of labile oxygen functional groups. For rGO, the mass loss at around 200 °C is only about 10%, indicating the efficient reduction of GO. For Pd/GO, the TG curve is similar to that of GO with a near 40% weight loss at about 200 °C. However, for Pd/rGO hydrogel, there is only about 17% weight loss in the range of 100–700 °C, indicating both the efficient reduction of GO and the embedded with Pd nanoparticles inside the 3D architecture. Elemental analysis experiment was also carried out to give the accurate context of the main elements, and the result reveals that it contains of 70.75% of carbon, 2.0% of hydrogen and 0.13% of nitrogen, and the result is consistent with that of the EDX analysis.

Fig. 5 shows the X-ray diffraction (XRD) profile of the 3D Pd/rGO hydrogel. For Pd nanoparticles, two diffraction peaks appear at 40° and 46°, which can be indexed to the Pd(111) and Pd(200) planes, respectively. After the formation of hydrogel, there appears a new wide peak at around 22°. It reveals that after reduction the interlayer spacing of rGO sheets becomes to 0.39 nm, indicating the self-assembly of the rGO nanosheets for the formation of the hydrogel. The XRD experiment reveals that the success of formation or nanocomposite of Pd/rGO.

The nitrogen adsorption/desorption isotherm study shows that the dried Pd/rGO hydrogel is porous architecture. As shown in Fig. 6, the BET specific surface area of the Pd/rGO composite is about 44.2 $m^2\ g^{-1}$, and the value is a little smaller than that of pure rGO gel (117.0 $m^2\ g^{-1}$), indicating the existence of Pd nanoparticles decreases the surface area of the product. The nitrogen adsorption/desorption isotherm study (Fig. 6b) shows that the dried Pd/rGO hydrogel is mesoporous, and the pore size distribution lies in 2–100 nm range. The pore volume determined by the BJH method is 0.15 $cm^3\ g^{-1}$ of the product. Combined the result of SEM measurements, the porous structure of macropores and mesopores may benefit to the molecule diffusion to active sites with less resistance.

The catalytic activity of the 3D Pd/rGO architecture in the C–C bonds formation was investigated using the Suzuki–Miyaura coupling reaction of bromobenzene or iodobenzene with phenylboronic acid as showed in Scheme 2. The reaction was carried out in a mixed solvent of ethanol and water (1:1) under an inert atmosphere. Table 1 lists the yields of biphenyl under the catalysis of the Pd/rGO using different feed stocks. For bromobenzene, the yield is 83% with 100% selectivity (TOF of 123,148 h^{-1}), indicating an efficient catalytic activity of the as-prepared catalyst. The yield is much

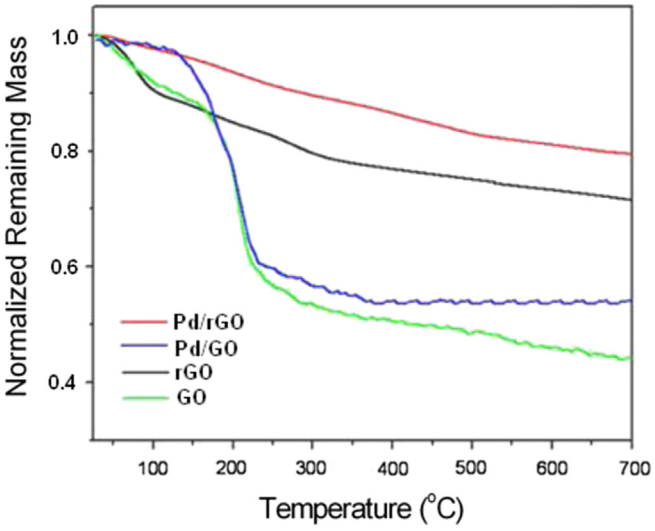

Fig. 4. TG curves of GO, rGO, Pd/GO, and the dried Pd/rGO hydrogels.

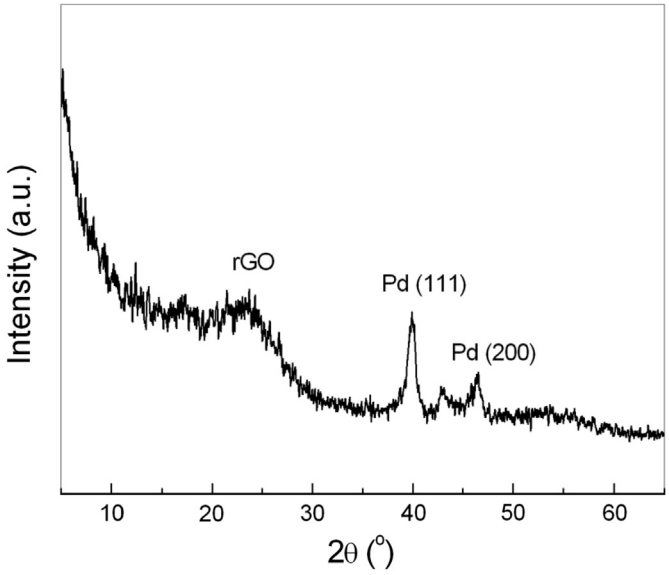

Fig. 5. XRD patterns of the dried Pd/rGO hydrogel.

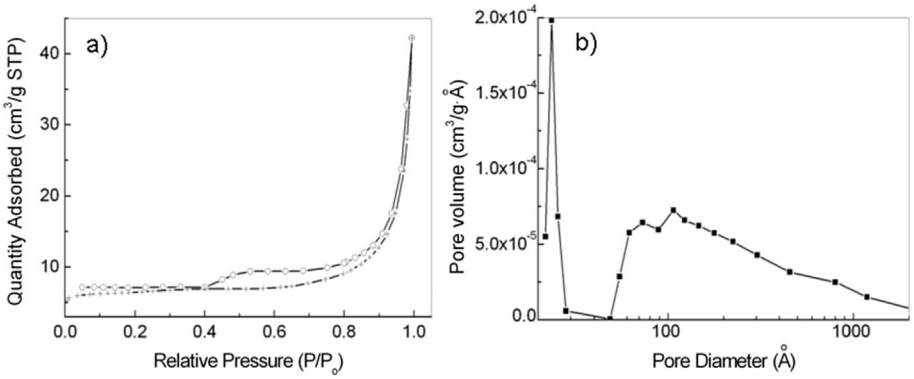

Fig. 6. N_2 adsorption/desorption isotherms (a) and pore size distribution (b) of the as-prepared dried Pd/rGO hydrogel.

Table 1
Catalytic activity of the Pd/rGO on the Suzuki–Miyaura coupling reaction of bromobenzene or iodobenzene.

Feed stocks	Yield (%)	Selectivity (%)
Bromobenzene	83.0	100
Iodobenzene	91.1	100

Table 2
The effect of reducing conditions of Pd nanoparticles formation on the yield of Suzuki–Miyaura reaction with bromobenzene or iodobenzene as feedstocks.

Reducing agent for Pd nanoparticles formation over GO nanosheets	Bromobenzene	Iodobenzene
Glycol	87.4%	100%
H_2 (30 min, 40 ml min^{-1})	61.6%	70.7%

higher than Pd/graphene hybrids catalyst prepared by reducing palladium acetate using sodium dodecyl sulfate (SDS) as both reducing agent and surfactant (the yield is 29.5% with 89.8% selectivity) [26]. When iodobenzene was used as feed stock, the yield reached 91.1% with 100% selectivity (TOF of 135,166 h^{-1}), which can be attributed to the week bond strength of C–I than that of C–Br and the electro-withdrawing ability of C–I group of the halogen substitution is higher.

Different reducing agents such as glycol or hydrogen gas for palladium nanoparticles formation had been studied [20] and after the formation of 3D Pd/rGO architectures, and their catalytic activities for C–C coupling reaction were studied, and Table 2 lists the yield of biphenyl with different catalysts. It reveals that both glycol and hydrogen are efficient reducing agents for the preparation of the catalysts, especially for glycol, and the yield was 100% when iodobenzene was used as feed stock.

It had been reported that the catalytic activity of Pd nanoparticles-graphene composite strongly depends on the size of the Pd nanoparticles, and the smaller Pd nanoparticles in size below 10 nm favor the higher catalytic activity for C–C coupling reactions [21]. Here, for the Pd/rGO prepared by reduction using

Table 3
Recycling experiment with Pd/rGO.

Run	Yield (%)
1	91.1
2	91.8
3	98.2
4	100

Table 4
Coupling of 4-methoxypheneboronic acid and 4-bromo-1,2-(methylene dioxy) benzene over Pd/rGO at different temperature.

Temperature (°C)	RT	60	80
Yield (%)	45	74	86

Vitamin C, the size of Pd particles is about 5–9 nm, which made the nanocomposite a good catalyst for Suzuki–Miyaura coupling reaction. The reaction mechanism studies revealed that there exists a dissolution–redeposition mechanism, and it is a widespread hypothesis that Pd nanoparticles function as a reservoir for the catalysis, and only a small amount of metal goes into solution as Pd^0 atoms and completion of the transformation. So the redeposition of Pd^0 nanoparticles onto the surface of support is a key factor to reverse the catalytic activity and cycling properties of the catalyst, and the 3D structure of graphene could prevent losing of Pd nanoparticles that in the 2D Pd/graphene system. Table 3 lists the catalytic activity of the catalyst in recycling experiments, and the activity slightly rose in the four runs, and the yield reached 100% for the fourth run. The catalyst also showed good catalysis activity when different substrates were used, such as the reaction between 4-methoxypheneboronic acid and 4-bromo-1,2-(methylene dioxy) benzene. As shown in Table 4, the yields increased with the increasing of reactive temperature.

4. Conclusions

3D Pd/rGO architectures had been prepared by the reduction of Pd^{2+} and growth of Pd nanoparticles over GO nanosheets followed a reduction-inducing self-assembly of the Pd/GO using Vitamin C. It can be used as catalyst for C–C bond coupling reaction. The result revealed that the 3D Pd/rGO is alternative to commercial Pd/C catalyst, and the as-prepared Pd/rGO showed high catalytic activity for Suzuki–Miyaura coupling reaction.

Acknowledgment

This work is supported by the National High Technology Research and Development Program (No. 2012AA051803 and 2012BAI27B05-2), and the National Basic Research Program of China (No. 2011CB921403 and 2010CB923302).

Appendix A. Supplementary data

Supplementary data related to this article can be found at http://dx.doi.org/10.1016/j.matchemphys.2014.07.018.

References

[1] J. Zhu, A. Holmen, D. Chen, ChemCatChem 5 (2013) 378–401.
[2] V. Sridhar, H.J. Kim, J.H. Jung, C. Lee, S. Park, I.K. Oh, ACS Nano 6 (2012) 10562–10570.
[3] W. Ren, Y.X. Fang, E.K. Wang, ACS Nano 5 (2011) 6425–6433.
[4] K.S. Novoselov, A.K. Geim, S.V. Morozov, D. Jiang, Y. Zhang, S.V. Dubonos, I.V. Grigorieva, A.A. Firsov, Science 306 (2004) 666–669.
[5] A.K. Geim, Science 324 (2009) 1530–1534.
[6] C.Z. Zhu, S.J. Dong, Nanoscale 5 (2013) 1753–1767.
[7] D.Q. Wu, F. Zhang, H.W. Liang, X.L. Feng, Chem. Soc. Rev. 41 (2012) 6160–6177.
[8] C. Li, G.Q. Shi, Nanoscale 4 (2012) 5549–5563.
[9] K.W. Chen, L.B. Chen, Y.Q. Chen, H. Bai, L. Li, J. Mater. Chem. 22 (2012) 20968–20976.
[10] Y.X. Xu, Z.Y. Lin, X.Q. Huang, Y. Liu, Y. Huang, X.F. Duan, ACS Nano 7 (2013) 4042–4049.
[11] W.J. Zhou, X.H. Cao, Z.Y. Zeng, W.H. Shi, Y.Y. Zhu, Q.Y. Yan, H. Liu, J.Y. Wang, H. Zhang, Energy Environ. Sci. 6 (2013) 2216–2221.
[12] X.H. Cao, Z.Y. Zeng, W.H. Shi, P.R. Yep, Q.Y. Yan, H. Zhang, Small 9 (2013) 1703–1707.
[13] W.F. Chen, S.R. Li, C.H. Chen, L.F. Yan, Adv. Mater. (Weinheim Ger.) 23 (2011) 5679.
[14] B.F. Machado, P. Serp, Catal. Sci. Technol. 2 (2012) 54–75.
[15] B. Adhikari, A. Biswas, A. Banerjee, ACS Appl. Mater. Interfaces 4 (2012) 5472–5482.
[16] W.F. Chen, L.F. Yan, Nanoscale 2 (2010) 559–563.
[17] P. Huang, W.F. Chen, L.F. Yan, Nanoscale 5 (2013) 6034–6039.
[18] Z. Jin, D. Nackashi, W. Lu, C. Kittrell, J.M. Tour, Chem. Mater. 22 (2010) 5695–5699.
[19] S.-H. Kim, G.H. Jeong, D. Choi, S. Yoon, H.B. Jeon, S.-M. Lee, S.-W. Kim, J. Colloid Interface Sci. 389 (2013) 85–90.
[20] C.C.C. Johansson Seechurn, M.O. Kitching, T.J. Colacot, V. Snieckus, Angew. Chem. Inter. Ed. 51 (2012) 5062–5085.
[21] G.M. Scheuermann, L. Rumi, P. Steurer, W. Bannwarth, R. Mülhaupt, J. Am. Chem. Soc. 131 (2009) 8262–8270.
[22] S. Moussa, A.R. Siamaki, B.F. Gupton, M.S. El-Shall, ACS Catal. 2 (2012) 145–154.
[23] G.J. Wu, X.M. Wang, N.I.J. Guan, L.D. Li, Appl. Catal. B Environ. 136 (2013) 177–185.
[24] A.R. Siamaki, A.E.S. Khder, V. Abdelsayed, M.S. El-Shall, B.F. Gupton, J. Catal. 279 (2011) 1–11.
[25] X.M. Chen, G.H. Wu, J.M. Chen, X. Chen, Z.X. Xie, X.R. Wang, J. Am. Chem. Soc. 133 (2011) 3693–3695.
[26] Y. Li, X.B. Fan, J.J. Qi, J.Y. Ji, S.L. Wang, G.L. Zhang, F.B. Zhang, Nano Res. 3 (2010) 429–437.
[27] S. Jafar Hoseini, M. Dehghani, H. Nasrabadi, Catal. Sci. Technol. 4 (2014) 1078–1083.
[28] S.S. Shendage, A.S. Singh, J.M. Nagarkar, Tetrahedron Lett. 55 (2014) 857–860.
[29] Ö. Metin, S. Ho, C. Alp, H. Can, M. Mankin, M. Gültekin, M. Chi, S. Sun, Nano Res. 6 (2013) 10–18.
[30] N. Li, Z. Wang, K. Zhao, Z. Shi, S. Xu, Z. Gu, J. Nanosci. Nanotechnol. 10 (2010) 6748–6751.
[31] L.J. Wu, Y. Wang, Y.P. Wang, X. Du, F. Wang, Y.Y. Gao, T. Qi, C.M. Li, RSC Adv. 3 (2013) 5196–5203.
[32] W. Chen, L. Yan, P.R. Bangal, Carbon 48 (2010) 1146–1152.